CSIRO PUBLISHING

www.publish.csiro.au/journals/ijwf *International Journal of Wildland Fire* **2010**, *19*, 163–170

An examination of fire spread thresholds in discontinuous fuel beds[A]

Mark A. Finney[A,B], *Jack D. Cohen*[A], *Isaac C. Grenfell*[A] *and Kara M. Yedinak*[A]

[A]USDA Forest Service, Rocky Mountain Research Station, Fire Sciences Laboratory, Fire Behavior, 5775 Highway 10 West, Missoula, MT 59808, USA.

[B]Corresponding autor. Email: mfinney@fs.fed.us

Abstract. Many fuel beds, especially live vegetation canopies (conifer forests, shrub fields, bunch-grasses) contain gaps between vegetation clumps. Fires burning in these fuel types often display thresholds for spread that are observed to depend on environmental factors like wind, slope, and fuel moisture content. To investigate threshold spread behaviours, we conducted a set of laboratory burn experiments in artificial fuel beds where gap structure, depth, and slope were controlled. Results revealed that fire spread was limited by gap distance and that the threshold distance for spread was increased for deeper fuel beds and steeper slopes. The reasons for this behaviour were found using a high-speed thermal camera. Flame movements recorded by the camera at 120 Hz suggested fuel particles experience intermittent bathing of non-steady flames before ignition and that fuel particles across the gap ignited only after direct flame contact. The images also showed that the flame profile within the fuel bed expands with height, producing greater horizontal flame displacement in deeper beds. Slope, thus, enhances spread by increasing the effective depth in the uphill direction, which produces wider flames, and thereby increases the potential flame contact. This information suggests that fire spread across discontinuous fuel beds is dependent on the vertical flame profile geometry within the fuel bed and the statistical properties of flame characteristics.

Introduction

Homogeneity is a property of wildland fuel beds that is frequently desired for purposes of experimentation and modelling of fire spread (Anderson 1964; Rothermel 1972; Weber 1991). Fuel beds that are homogeneous in particle sizes and packing are not physically continuous because they are composed of individual fuel particles and interstitial air spaces (Fons 1946). Even at the fine intraparticle scales found in natural pine-needle fuel beds or artificial matchstick arrays, separation of particles has been demonstrated to produce threshold conditions for fire spread (Vogel and Williams 1970; Weber 1990). When spread is at or near this threshold, the insufficiency of total heat transfer presents an opportunity to gain insight into what mechanisms are necessary and sufficient for ignition and spread.

In nature, many fuel beds give the appearance of being uniform and continuous because the gaps between particles are very small (e.g. pine-needle beds and some grasslands). Other fuel types display discontinuities between individual plants rather than particles, for example live vegetation canopies (conifer forests, shrub fields, bunch-grasses). Fires burning in these live fuels often display thresholds for horizontal spread that are observed to depend on environmental factors like wind and fuel moisture content (Van Wagner 1977; Brown 1982; Bradstock and Gill 1993; Cheney *et al*. 1998; Marsden-Smedley *et al*. 2001, Weise *et al*. 2005). The present paper describes the results of laboratory fire experiments involving artificial fuel beds that were constructed with horizontal discontinuities to specifically examine thresholds in fire spread and investigate physical mechanisms to explain this behaviour.

Experimental apparatus and methods

The experimental design examined thresholds of fire spread in terms of three variables: vertical fuel-bed depth, horizontal spacing between fuel elements, and slope. A fuel 'element' consisted of medium-grade excelsior (surface area to volume ratio $\sim$7590 m^{-1}) spun around a metal rod to a 15-cm diameter (Fig. 1). Excelsior was chosen to facilitate repeatability of the experiments and not to be associated with any particular natural fuel type. However, for purposes of comparison, the surface area-to-volume ratio of medium-grade excelsior particles is similar to that measured for natural fuel particles including some grasses and pine needles (Brown 1970; Fernandes and Rego 1998). The desired depth of the fuel bed could be adjusted at intervals of 15 cm between fuel supports (wire tines of length 15 cm) soldered onto the rod (we used depths of 30, 60 and 120 cm). Lineal fuel loading on each rod was held constant at 97 g of dry excelsior per metre of depth (5.489 kg m^{-3} bulk density). A platform 1.2 × 4.8 m (4 × 16 feet) was used for all fuel beds and contained rows of metal cross-members at 5-cm spacing along the long-axis of the bed (*x*-direction). Holes drilled in each cross-member supported the fuel elements vertically (Fig. 1). Fuel elements were arranged on a rectangular grid with a fixed

[A]The manuscript was produced by US Government employees on official time and is therefore in the public domain and subject to copyright laws in the US.

10.1071/WF07177 1049-8001/10/020163

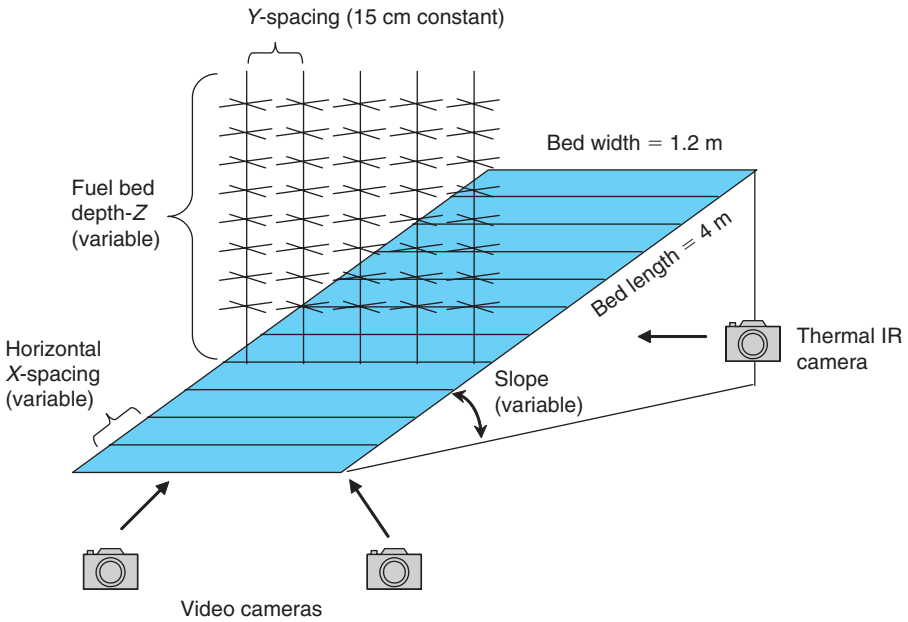

Fig. 1. Schematic of the experimental setup showing the platform on which discontinuous fuel beds were built by arranging vertical fuel rods with varying horizontal spacing and depths (1.2 by 4.8 m).

15-cm spacing in the *y*-direction (short axis of the bed) and variable spacing (at 5-cm resolution) in the *x*- or longitudinal direction. The cross-members could be rotated (*x*–*z* plane) to maintain the vertical orientation of the fuel elements when the platform was tilted.

A suite of experimental burns was conducted for the purpose of identifying fire spread thresholds. Environmental conditions were held approximately constant at 27°C (80°F) and 80% relative humidity for ~4 to 5 h before burning. Fuel moisture was estimated from two 50-g samples of excelsior removed from the fuel bed immediately before burning. Samples were weighed before and after oven-drying at 60°C for 24 h and moisture content calculated on a standard dry-weight basis. Ignition of a full flame zone was accomplished by spraying ethanol along the base of the short axis of the platform and immediately lighting it. Flames spread vertically up the first row of elements and then along the *x*-axis of the fuel bed (Fig. 1).

The spread threshold for a combination of fuel-bed depth and horizontal spacing was found experimentally with a series of burns at increasingly steep slopes. For successive burns, the slope was increased until the fire was able to spread the entire length of the fuel bed. At least three replications were attempted for each setting, with more conducted for areas appearing near the threshold. Burns were classified as 'successful' if the fire burned the entire length of the bed and produced a steady sequence of ignition of each row, 'marginal' if the fire spread the length of the bed but demonstrated non-steady ignition of at least one row or continuance only by spotting, and 'unsuccessful' if fire did not spread the entire length of the bed. Experiments were only conducted near the threshold and not for the full range of variables possible in the experiment.

A digital thermal camera provided image samples of the flame behaviour as the fire spread past the centre of the *x*-dimension of the fuel bed (well beyond any influence of the ignition). The thermal infrared camera (TVS-8500, by Cincinnati Electronics, Mason, OH[B]) was aimed at a fixed cross-section of the fuel bed normal to the nadir of the field of view. The cooled detectors of the focal plane array in the camera are capable of capturing independent sequential images at the 120-Hz sampling rate within the factory-calibrated range of temperature (−40° to 900°C). An 8-s sample period provided 1024 thermal images at a rate of 120 Hz as the flame crossed the viewing plane. Standard digital video cameras provided a visible record from two vantage points in the combustion chamber (Fig. 1).

The digital images from the thermal camera were analysed by converting raw digital sensor readings ('counts') in each pixel to an approximate temperature. Accurate flame temperature is difficult to determine on thermal images because of the low emissivity of flame gases and confusion of the signature with the cooler background. Thus, based on the subjective threshold of 550°C, the images were converted to binary flame presence (0 or 1) and time-integrated to display the probability distribution over the 8-s burst. No attempt was made to correct the images for actual *x*–*y* position of the pixels (Fig. 1). The flame front achieved a typical bowed or curved shape in the horizontal plane (*x*–*y*). Fortuitously, this convex front diminishes parallax from the *y*-direction and facilitates the interpretation of the frontal characteristics directly from the images.

Linear regressions were performed to characterise the spread thresholds for fuel-bed depth categories (30, 60, 120 cm deep). The dependent variable was the 'effective fuel-bed depth' ($depth + gap \times \sin(slope)$) as predicted by a given actual

[B]Tradenames are provided for informational purposes only and do not constitute endorsement by the USDA.

Table 1. Summary of data from experimental burns
Data used for regression analysis of the fire spread threshold location excluded settings where replications produced uniformly successful or unsuccessful spread responses

Fuel depth (cm)	Gap (cm)	Slope (degrees)	Number of experiments	Data used in threshold regressions
30	20	9–18	2	2
30	25	24–30	5	5
30	30	3–39	5	3
60	20	0	1	0
60	25	0–24	12	10
60	30	0–30	7	5
60	35	15–33	15	10
120	25	0–33	9	8
120	30	9–30	37	28
120	35	3–27	12	6
120	40	24–33	7	7
Total			112	84

horizontal gap distance ($gap \times \cos(slope)$), where the 'gap' represents the separation distance between fuel rows as measured parallel with the surface plane of the platform. Data used for the regressions were from all settings of the fuel bed (slope and depth and gap spacing) where spread responses (spread or no spread) varied among replications, i.e. near the spread threshold (Table 1). Thus, data from fuel-bed settings that produced consistently 'successful' or 'unsuccessful' spread responses were not included in these regressions because the ranges of fuel-bed settings above or below the unknown threshold (those that would always burn or always not burn) were not controlled.

Results

A total of 112 experiments were conducted with different combinations of depth, spacing, and slope (Table 1). Ignition of excelsior particles across fuel-bed gaps was observed to be dependent on flame contacts evident in visible video images and in thermal images with flame gases having a black-body emissive temperature of at least 550°C. The visible and infrared cameras showed that flame eddies rising along the leading edge of the front were responsible for spanning the gaps between rows (Fig. 2). Ignition of fuel particles by flame contact could be clearly seen in slow-motion sequences of thermal images taken at 120 Hz and visible images at 30 Hz. In some experiments where fire did not spread or was considered marginal, embers detached from the glowing fuel particles and drifted into the fresh excelsior, resulting in ignition. Ignition did not occur without either flame contact or ember ignition.

The vertical profiles of the flames at the combustion interface within the fuel bed were found to have a curved shape that was inclined with positive slope into the unburned portion of the fuel bed (Fig. 3). Parallax in the *y*-dimension was minimal because the curved shape of the front in the *x*–*y* plane allowed the leading edge of the fire (middle of the *y*-plane) to be viewed without interference from flames in the foreground or background. The temporal variability of the flame edge was investigated by time-averaging the 120-Hz images after coding each frame

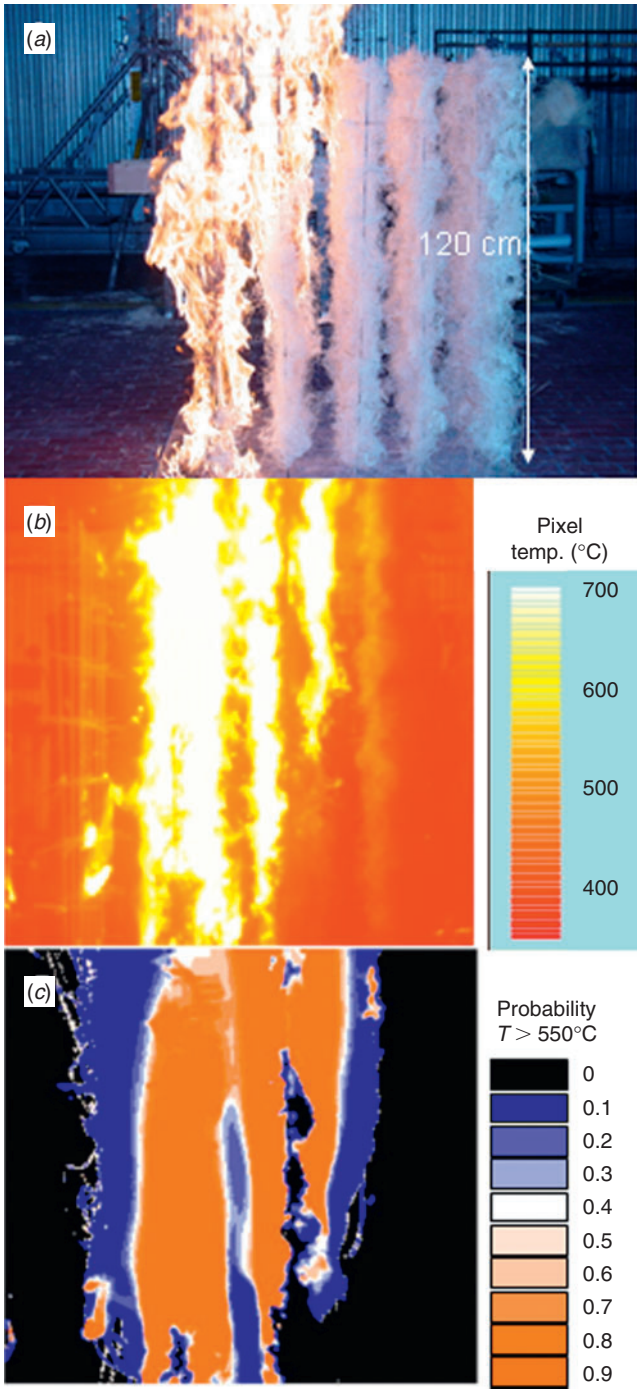

Fig. 2. Images of an experimental fire burning left to right across a discontinuous fuel bed. Visible image (*a*) and thermal image (*b*) show non-steady flame behaviour at the leading edge of the fire. This non-steady flame behaviour was characterised by a probability of flame presence (temperature greater than 550°C) over 8 s of 120-Hz thermal images.

to distinguish flame presence and absence (Fig. 4). The time-averaged flame presence over the ~8-s time-span suggested that cross-sections of the flame edge could be characterised by a probability density function (PDF) of distance into the flame.

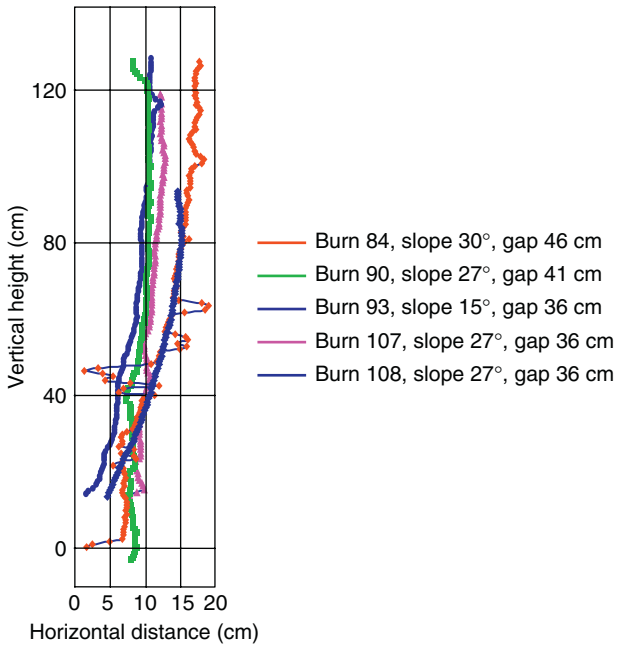

Fig. 3. Average flame positions in the x–z cross-section from five burns in 120 cm-deep fuels (different colours for each burn) suggest a curving combustion interface develops within the fuel bed.

A Kolmogorov–Smirnov test failed to reject tests that these probability distributions were Gaussian using the empirically determined variances.

These PDFs were also found to increase in variance with height (Fig. 4). Thus, for each height position, we derived an estimate of the variance of flame excursion. Confidence intervals for these variances were obtained via Christensen (1998, p. 56). The formula used gives the lower bound for each confidence interval as $((n-1)s^2)/(\chi^2(1-\alpha/2,n-1))$ and the upper bound as $((n-1)s^2)/(\chi^2(\alpha/2,n-1))$, where n is the number of pixel elements in the given height slice, s^2 is the estimated variance, and α is the significance level of the comparison (we used $\alpha = 0.9$). As the upper bound of the confidence intervals at the lower heights was less than the lower bound at the higher heights, we concluded that there was a significant increase in variance with respect to height.

As the leading edge of the flame advanced across a given pixel in the image, the non-steadiness of the flames could be characterised as an intermittent flame signal (Fig. 5). Flame presence in a pixel (temperature >550°C, depicted as blue bands in Fig. 5) shows greater intermittency closer to the unburned fuel (farther from the continuous flame zone) throughout the 8-s time-series of thermal images. This intermittency appeared to be related to the variable sizes of flame eddies that occur over time, as suggested by the coincidence of flame presence in adjacent pixels (Fig. 5). Flame eddies with larger diameter extended across many pixels, starting proximal to the continuous flame and extending to more remote pixels at a particular vertical level (Fig. 5). Smaller eddies only crossed the camera pixels closer to the more continuous flame zone.

Regression analysis of the fire spread thresholds suggested wider horizontal spacing could be breached with steeper slopes as indicated by the positive slope of the regression lines for each fuel-bed depth setting (Table 2, Fig. 6). Breaching of horizontal gaps occurred at flatter slopes in deeper beds (Table 2, Fig. 6). Examination of flame video revealed that the fire spread downward from the top of the bed at a rate of $\sim$1.5 m min^{-1} (0.025 m s^{-1}) and produced a vertical depth of the combustion zone consistently from 45 to 60 cm deep. Flame residence times at a particular x, y, z point were therefore between 18 and 24 s.

Discussion

Ignition of fuel particles after direct contact with visible flames was found to be the essential mechanism by which our laboratory fires propagated across discontinuities in excelsior fuels. The thermal images clearly showed fuel particle ignitions only after flame bathing. This implies that the net radiation heating was not sufficient for fire spread. The observation that non-steady flames are responsible for the horizontal extension of flames critical for convective fuel-bed heating has been noted for many years. Hottel *et al.* (1965) and Emmons (1965) proposed a Gaussian probability distribution of horizontal flame extensions similar to our findings here. Albini (1967) speculated that 'small-scale flame deflections by wind and turbulence may produce flame bathing of the unburned fuel and contribute directly to flame attachment and spread rate'. Anderson (1969) concluded that 'convective heat transfer must be the primary source [of propagating heat flux] through some horizontal transport mechanism'. Beer (1990) documented advective preheating of fuel by direct flame contact ahead of the combustion zone and within fuel beds of vertical matchsticks. Fendell and Wolff (2001) formulated a critical wind speed in discontinuous fuels for bending flames and producing direct flame contact. Nelson and Adkins (1987) asserted that 'the key process in spread of the wind-driven fire is horizontal displacement of flame at the fuel surface' and conjectured that the same formula responsible for fire spread occurs in surface and crown fires. Baines (1990) concluded that flame variability from wind and turbulence was critical to fire movement. All of these observations would suggest, as did Steward (1971), a statistical rather than deterministic interpretation of small-scale convection for purposes of fire modelling.

The curved shape of the fire front was similar to that in previous studies that reported shapes of the combustion interface within the fuel bed. Our experimental fuel beds were much deeper (up to 1.2 m), but Vogel and Williams (1970) described a fourth power 'flame standoff' function of radial distance from individual fuel particles. Weber (1990) utilised a cubic function of distance from a fuel particle for a laminar flame profile in matchsticks, and Albini (1985, 1986) found curved shapes of ignition interfaces in shallow fuel beds empirically and theoretically. Yedinak *et al.* (2010) described a model for laminar flame profiles from a stationary source that closely correspond to the shape of the ignition interface found in our spreading fires. In our experiments, however, the flame structure was not laminar and ignitions occurred by fleeting contact with intermittent flames rather than a steady flame boundary. The non-steady edge of the flame profile within the fuel bed contributed to successful fire spread by increasing the horizontal displacement of the flames across gaps and into the unburned fuel.

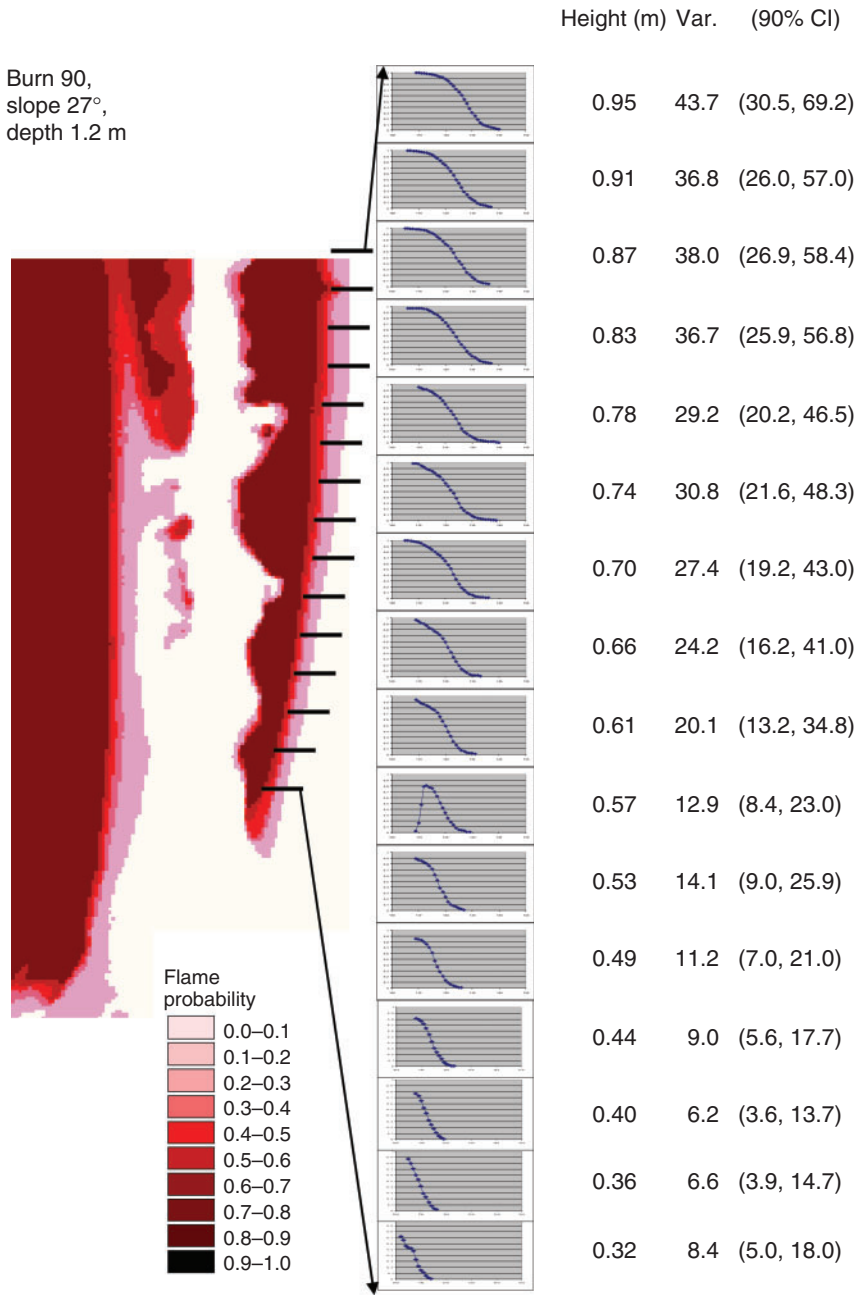

Fig. 4. Sample distributions of flame presence recorded at different heights on the advancing edge of one experimental fire (fuel-bed depth was 1.2 m, fire moving from left to right up a slope of 27°). The image was obtained by time-averaging the thermal images of flame presence (temperature greater than 550°C) over 8 s at 120 Hz. White regions within the shades of red indicate an absence of flame visible to the camera behind foreground fuel elements (see Fig. 1). The empirical distributions are statistically indistinguishable from Gaussian and their variances increase significantly with height as indicated by overlapping 90% confidence intervals (CI).

Flame and fuel geometry appeared to play a strong role in determining successful spread in these experiments. As observed by Vogel and Williams (1970), Fang and Steward (1969), and Weber (1990), wider gaps between fuel elements decreased flame contacts and consequent spread. Weber (1990) demonstrated an effect of steeper slopes that allowed the fire to cross gaps because the increasing effective depth of the fuel bed (uphill elements are raised higher) puts the top of the fuel bed in contact with a wider flame profile. Our experiments produced results similar to Weber (1990), despite having much deeper

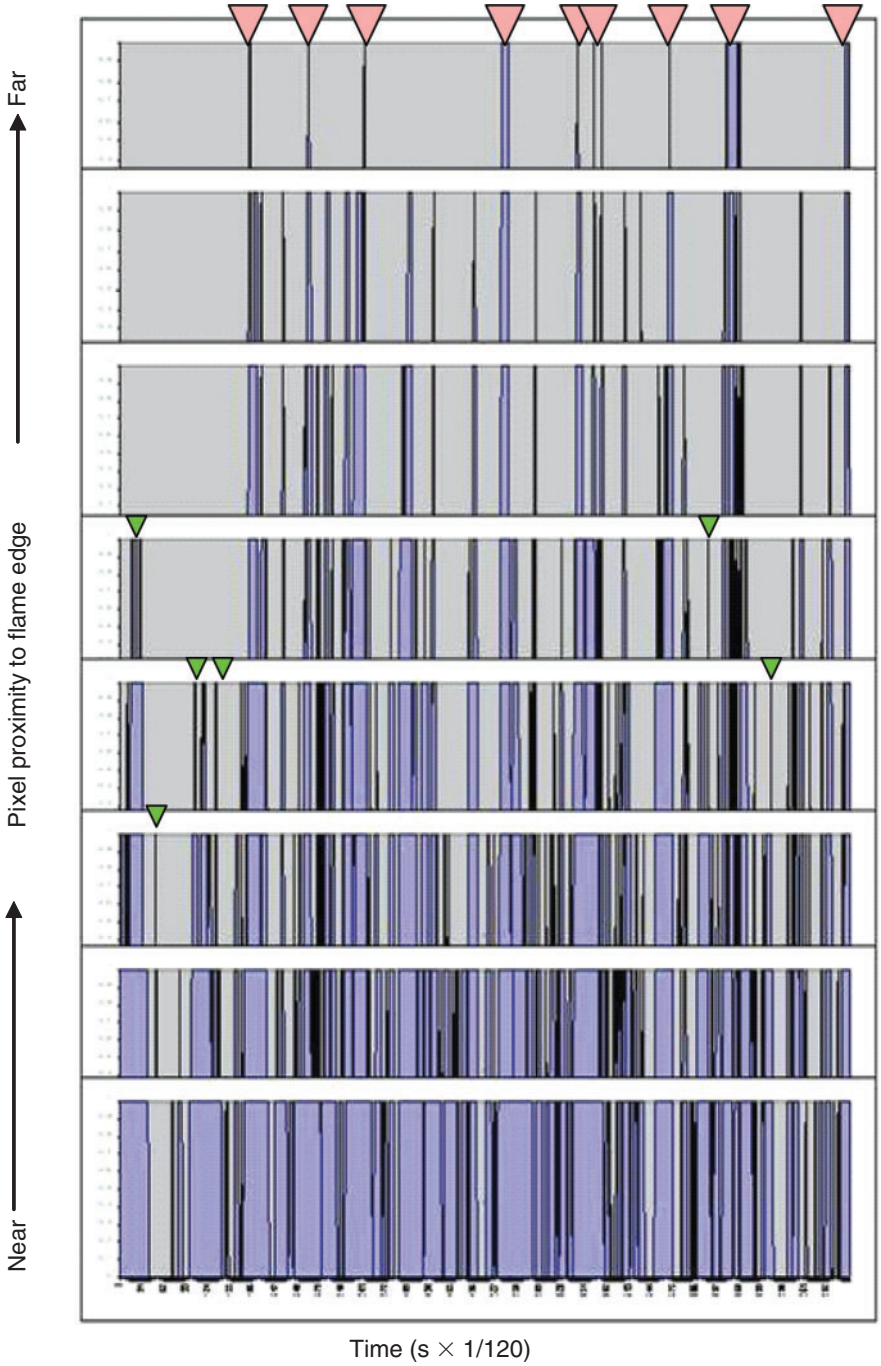

Fig. 5. Time-series of flame presence signals (pixel temperature greater than 550°C) compared for a horizontal transect of pixels across the flame edge at 120 Hz (total time is 8 s). Blue bands indicate presence of flame in the pixel. These signals show increasing intermittency of flames at pixel locations farther from time-averaged leading edge of the fire. The largest eddies are represented by bands farthest from the flame edge and are indicated with a red triangle. Smaller eddies extend for shorter distances and are indicated by small green triangles. Wider blue bands along the time-axis indicate longer durations of flame presence. Data from this example are from an experiment with slope of 27° in a fuel bed 1.2 m deep. Note that flames recorded at positions far from the edge tend to be recorded simultaneously across all closer positions because the eddy structure extends outward from the continuous flame zone.

Table 2. Summary of linear regression results that were used to evaluate fire spread threshold responses (see Fig. 6)

Fuel depth (cm)	Intercept	Slope coefficient	*n*	Standard error	r^2
30	−3.172	2.247	10	1.064	0.736
60	20.911	0.641	25	1.663	0.264
120	40.903	0.896	49	1.968	0.275

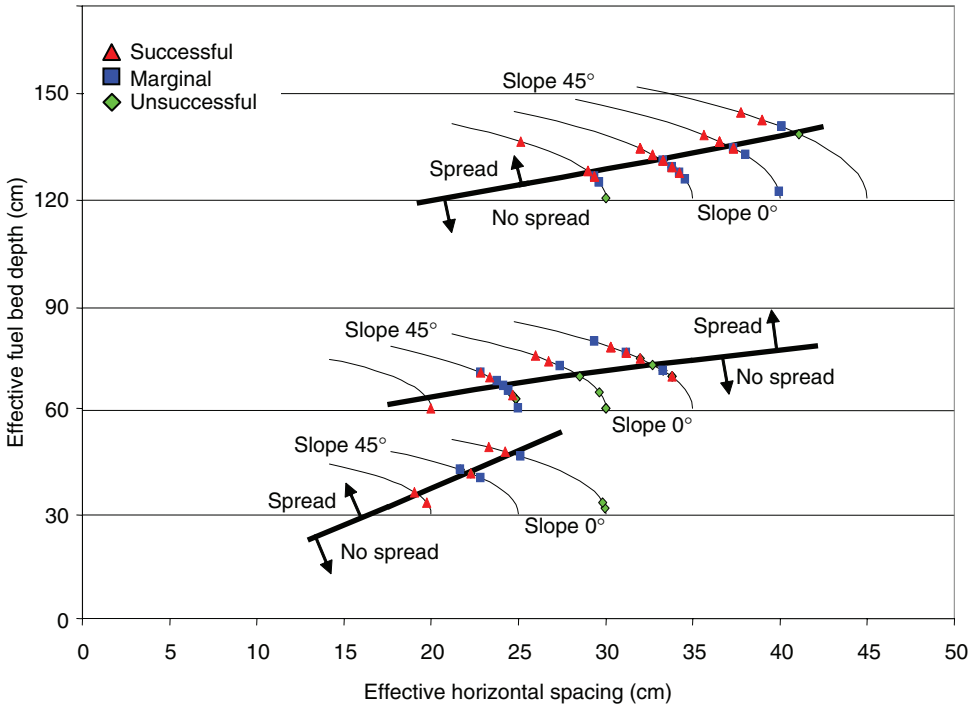

Fig. 6. Regression thresholds for spread in discontinuous fuel beds (bold black lines) are plotted by effective fuel-bed depth ($Z + gap \times \sin(slope)$) and effective horizontal spacing ($gap \times \cos(slope)$) where the 'gap' represents the separation distance between fuel rows as measured parallel with the surface plane of the platform (see Table 1 for summary of experimental data and Table 2 for regression statistics). For a given fuel depth category, experimental fires would successfully spread above these thresholds but not spread below them. Deeper beds and narrower horizontal gaps facilitated spread. The potential range of experimentally controlled variables is indicated by the curving fine lines that delineate effect of slope changes (0° to 45°) for the depth and spacing combinations. Coloured points represent the results of individual burns in terms of their success in producing fire spread the entire length of the bed (see text under Methods).

beds and turbulent flames. We found spread occurred in deeper beds at wider horizontal spacing even when the total fuel-bed depth exceeded the observed maximum combustion depth of 45 to 60 cm. Expansion of the flame profile above the upper edge of the fuel bed can occur because flame eddies are still increasing in size, as indicated by the higher variance of the flame edge with height above the ground (Figs 2, 4). In the shallowest fuel beds (30 cm), however, the regression analysis suggested a steeper slope coefficient for the threshold response to gap distance than in the deeper fuel beds (Table 2, Fig. 6), likely because the fuel-bed depth restricted the combustion zone to less than the maximum 45 to 60 cm found in deeper beds.

Irrespective of the exact threshold locations in these experiments, our results do not support the hypothesis that bulk properties of fuel beds, for example crown bulk density (Van Wagner 1977), determine fire spread where fuel discontinuities exist. Bulk density was constant for a given horizontal gap spacing, yet thresholds associated with a given gap were breached as the fuel depth increased.

The evidence of the curved combustion interface shape is suggestive of a physical explanation for the long-observed elliptical shapes of wildland fires on slopes and in the presence of wind (Peet 1967; Van Wagner 1969; Anderson 1983; Alexander 1985). If the combustion interface were symmetric in the *x*–*y* plane, as in a surface of revolution around the *z*-axis (e.g. a cone or paraboloid), mathematical ellipses would result from non-normal sections through the contained volume. Sloping ground would produce such elliptical sections in these experiments if

the flame profile were symmetric in 360 degrees, even with constant horizontal rates of fire movement. This implies that flanking and backing fire spread rates or thresholds could be directly estimated as a function of angles around the volume. If a wind should solely result in a tilting of the volume, ellipses would result from a horizontal section, but we have yet to extend our experiments to a wind tunnel to see what interface shapes evolve under presence of cross-flow.

Conclusions

For our no-wind experiments in discontinuous fuelbeds, fire spread occurred only after ignition by direct flame contact. The vertical flame profile within the fuel bed was observed to expand with height, in part because flame eddies became larger as they rose along the leading edge of the fire. Thus, non-steady flames extended farther across fuel gaps in deeper or effectively deeper (slope) fuel beds to make fuel contacts and produce ignitions. Fires were more likely, therefore, to spread in deeper beds and on steeper slopes. This has broad implications for approaches to modelling of fire spread, the importance of convection, and the characterisation of flames in both continuous and discontinuous fuel types.

Acknowledgements

The authors are indebted to Bob Schuette who led the design and construction of laboratory equipment, Paul Sopko for help with instrumentation and environmental conditioning, and AJ Hershman and DK Paige and numerous technicians who tirelessly built the fuel beds for the experiments.

References

Albini FA (1967) A physical model for firespread in brush. In 'Eleventh Symposium on Combustion', 14–20 August 1966, University of California, Berkeley. pp. 553–560. (The Combustion Institute: Pittsburgh, PA)

Albini FA (1985) A model for fire spread in wildland fuels by radiation. *Combustion Science and Technology* **42**, 229–258. doi:10.1080/00102208508960381

Albini FA (1986) Wildland fire spread by radiation – a model including fuel cooling by natural convection. *Combustion Science and Technology* **45**, 101–113. doi:10.1080/00102208608923844

Alexander ME (1985) Estimating the length-to-breadth ratio of elliptical forest fire patterns. In 'Proceedings of the Eighth Conference on Fire and Forest Meteorology', 29 April–2 May 1985, Detroit, MI. (Eds LR Donoghue, RE Martin) SAF Publication 85–04, pp. 287–304. (Society of American Foresters: Bethesda, MD)

Anderson HE (1964) Mechanisms of fire spread research progress report No. 1. USDA Forest Service Intermountain Forest and Range Experiment Station, Research Paper INT-8. (Ogden, UT)

Anderson HE (1969) Heat transfer and fire spread. USDA Forest Service, Research Paper INT-69.

Anderson HE (1983) Predicting wind-driven wildland fire size and shape. USDA Forest Service, Research Paper INT-305.

Baines PG (1990) Physical mechanisms for the propagation of surface fires. *Mathematical and Computer Modelling* **13**(12), 83–94. doi:10.1016/0895-7177(90)90102-S

Beer T (1990) The interaction of wind and fire. *Boundary-Layer Meteorology* **54**, 287–308.

Bradstock RA, Gill AM (1993) Fire in semi-arid Mallee shrublands: size of flames from discrete fuel arrays and their role in the spread of fire. *International Journal of Wildland Fire* **3**(1), 3–12. doi:10.1071/WF9930003

Brown JK (1970) Ratios of surface area to volume for common fine fuels. *Forest Science* **16**(1), 101–105.

Brown JK (1982) Fuel and fire behavior prediction in big sagebrush. USDA Forest Service, Intermountain Forest and Range Experiment Station, Research Paper INT-290. (Ogden, UT)

Cheney NP, Gould JS, Catchpole WR (1998) Prediction of fire spread in grasslands. *International Journal of Wildland Fire* **8**(1), 1–13. doi:10.1071/WF9980001

Christensen R (1998) 'Analysis of Variance, Design and Regression: Applied Statistical Methods.' (Chapman & Hall and CRC Press: Boca Raton, FL)

Emmons HW (1965) Fundamental problems of the free-burning fire. In 'Tenth Symposium (International) on Combustion', 17–21 August 1964, University of Cambridge, UK. pp. 951–964. (The Combustion Institute: Pittsburgh, PA)

Fang JB, Steward FR (1969) Flame spread through randomly packed fuel particles. *Combustion and Flame* **13**(4), 392–398. doi:10.1016/0010-2180(69)90108-4

Fendell FE, Wolff MF (2001) Wind-aided fire spread. In 'Forest Fires: Behavior and Ecological Effects'. (Eds E. A Johnson, K. Miyanishi) Ch. 6, pp. 171–223. (Academic Press: San Diego, CA)

Fernandes PM, Rego FC (1998) A new method to estimate fuel surface area-to-volume ratio using water immersion. *International Journal of Wildland Fire* **8**(2), 59–66. doi:10.1071/WF9980059

Fons WL (1946) Analysis of fire spread in light forest fuels. *Journal of Agricultural Research* **72**(3), 93–121.

Hottel HC, Williams GC, Steward FR (1965) The modeling of fire-spread through a fuel bed. In 'Tenth Symposium (International) on Combustion'. pp. 997–1007. (The Combustion Institute: Pittsburgh, PA)

Marsden-Smedley JB, Catchpole WR, Pryke A (2001) Fire modelling in Tasmanian buttongrass moorlands. IV Sustaining versus non-sustaining fire. *International Journal of Wildland Fire* **10**, 255–262. doi:10.1071/WF01026

Nelson RM, Adkins CW (1987) A dimensionless correlation for the spread of wild-driven fires. *Canadian Journal of Forest Research* **18**, 391–397.

Peet GB (1967) The shape of mild fires in Jarrah forest. *Australian Forestry* **31**(2), 121–127.

Rothermel RC (1972) A mathematical model for predicting fire spread in wildland fuels. USDA Forest Service, Intermountain Forest and Range Experiment Station, Research Paper INT-115. (Ogden UT)

Steward FR (1971) A mechanistic fire spread model. *Combustion Science and Technology* **4**, 177–186. doi:10.1080/00102207108952483

Van Wagner CE (1969) A simple fire growth model. *Forestry Chronicle* **45**, 103–104.

Van Wagner CE (1977) Conditions for the start and spread of crown fire. *Canadian Journal of Forest Research* **7**, 23–34. doi:10.1139/X77-004

Vogel M, Williams FR (1970) Flame propagation along matchstick arrays. *Combustion Science and Technology* **1**, 429–436. doi:10.1080/00102206908952223

Weber RO (1990) A model for fire propagation in arrays. *Mathematical and Computer Modelling* **13**(12), 95–102. doi:10.1016/0895-7177(90)90103-T

Weber RO (1991) Modelling fire spread through fuel beds. *Progress in Energy and Combustion Science* **17**, 67–82. doi:10.1016/0360-1285(91)90003-6

Weise DR, Zhou X, Sun L, Mahalingam S (2005) Fire spread in chaparral – 'go or no-go'. *International Journal of Wildland Fire* **14**(1), 99–106. doi:10.1071/WF04049

Yedinak KM, Cohen JD, Forthofer JM, Finney MA (2010) An examination of flame shape related to convection heat transfer in deep-fuel beds. *International Journal of Wildland Fire* **19**, 171–178. doi:10.1071/WF07143

Manuscript received 21 December 2007, accepted 11 November 2008